Propagation Characteristics of Compression Waves Reflected from the Open End of a Duct

Heuy Dong Kim*
School of Mechanical Engineering, Andong National University, 388, Songchun-dong, Andong 760-749, Korea
Dong Hoon Lee
Department of Mechanical Engineering, Seoul National University of Technology, 172, Kongneung-dong, Nowon 139-743, Korea
H. Kashimura
Department of Control and Information Systems Engineering Kitakyushu National College of Technology, Kitakyushu, 802-0985, Japan
T. Setoguchi
Department of Mechanical System Engineering, Saga University, 1, Honjo-machi, Saga 840-8502, Japan

The present study addresses the distortion of the compression wave reflected from an open end of a shock tube. An experiment is carried out using the simple shock tube with an open end. Computational work is also performed to represent the experimented flows. The second-order Total Variation Diminishing scheme is employed to numerically solve the unsteady, axisymmetric, inviscid, compressible governing equations. Both the experimented and predicted results are in good agreement. The generation and development mechanisms of the compression wave, which is reflected from the open end of the shock tube, are obtained in detail from the present computations. The effect of size of the baffle plate at the open-end that causes the reflection of the incident expansion wave is found negligible. A good correlation is obtained for transition of the reflected compression wave to a shock wave inside the tube. The present data show that for a given wave length of the incident expansion wave the transition of the reflected compression wave to a shock wave can be predicted with good accuracy.

Key Words : Compressible Flow, Unsteady Flow, Shock Wave, Compression Wave, Expansion Wave, Shock Tube

1. Introduction

The unsteady wave motions in a duct system are of practical importance in a variety of industrial pipe system. A pressure wave is usually produced by an on-off motion of valve, propagating along the pipe system, at an approximately same speed of sound of the working fluid. When the pressure wave meets the open end of a duct, it is reflected by the boundary conditions of the open end and propagates back along the duct, with an inverse phase to the incident pressure wave. The resulting wave may again reflect at a flow device in the duct system. Thus the wave reflection is repeated inside the duct system, leading to a pressure transient. (Kentfield, 1993 ; Kim et al., 2001) This problem is almost always associated with noise and vibration of a duct.

Some part of the pressure wave, which reaches

* Corresponding Author,
E-mail : kimhd@andong.ac.kr
TEL : +82-54-820-5622; **FAX** : +82-54-841-1630
School of Mechanical Engineering, Andong National University, 388, Songchun-dong, Andong 760-749, Korea. (Manuscript **Received** April 16, 2001; **Revised** February 17, 2003)

the open end of the duct, is discharged from the open end. The resulting wave usually reduces to a pulse wave, leading to an impulsive noise, (Raghunathan and Kim, 1998) which is recently a new type of environmental noise problem. The impulsive wave emitted from the open end of the duct has some characteristics like a direct current component of the incident pressure wave, while the pressure transient inside the duct is alike an alternative current component of the incident wave.

The pressure wave inside the duct essentially experiences attenuation and distortion during the propagation process inside the duct until it is faded down due to viscous friction and heat transfer effects. (Ogawa, 1997) A compression wave may become a shock wave due to a nonlinear character of the wave itself. (Kim, 1996) This transition process is not yet well understood. For instance, as a high-speed train enters a tunnel, a compression wave is generated ahead of the train and propagates along the tunnel. The compression wave would reflect back from the exit of the tunnel and propagates back toward the tunnel entrance, as an expansion wave. If the incident wave were expansion wave in character, then it would reflect back from the exit of the tunnel, as a compression wave. Such a situation is made inside the tunnel as the after body of a train enters the entrance of tunnel, recently being an important issue in the high-speed railway/train systems. (Kim et al., 2001 ; Matsuo and Aoki 1992)

Much work has devoted to attenuation and distortion mechanisms of the compression wave occurring during the propagation process. Ozawa et al. (1994) and Matsuo et al. (1996) have calculated the propagation processes of compression waves with a proper treatment of viscous friction and heat transfer effect and their prediction results are compared with the measured results in real high-speed railway tunnels. Sasoh et al. (1993) have discussed the distortion problem of the compression wave occurring ahead of a high-speed railway train and they have showed that the theoretical and computational predictions represent well the experimental results associated with the wave attenuation and distortions. But the transition characteristics from a compression wave to a shock wave during the propagation processes are, however, not well known.

Prediction of the transition from a compression wave to a shock wave is of practical importance from the point of view of a train body design and passengers in a train as well, since the shock wave would interference with the running train inside a tunnel. To the authors' knowledge, there is no work available to predict the transition problem. The present study has investigated the detailed mechanism of the wave transition process from a reflected compression wave toward a shock wave, both through a shock tube experiment and computation. An experiment has been carried out using a shock tube with an open end and generation and development processes of the compression wave, which reflects back from the open end of the shock tube, are measured using a pressure transducer, flush mounted on the shock tube wall. Computations have performed to represent the experimental result using the unsteady, axisymmetric, Euler's equations.

2. Experimental Work

The simple open-ended shock tube has a diameter (D) of 66 mm and a total length of about 4.44 m (the length of the driven section : 2.52 m), as shown in Fig. 1. A sheet of cellophane with 0.03 mm thick is used as a diaphragm, which is manually ruptured to initiate the wave motion. The initial pressure ratio p_1/p_4 of the shock tube is set to obtain the expansion wave in the driver section, which has an open end of the shock tube. The expansion wave, which are generated by sudden rupture of the diaphragm, propagates downstream toward the open end of the shock tube and then is reflected as the compression wave from the open end of the shock tube, as schematically shown in Fig. 2. To obtain this flow, the initial pressure ratio p_1/p_4 is set to be less than 1.0, where p_1 is the pressure in the driver section and p_4 the pressure in the driven section. In the present experiment, p_1 is kept constant at atmospheric pressure.

At the open end of the shock tube, a baffle plate

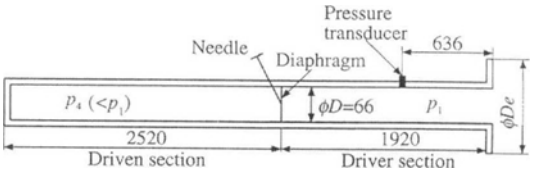

Fig. 1 Open ended shock tube

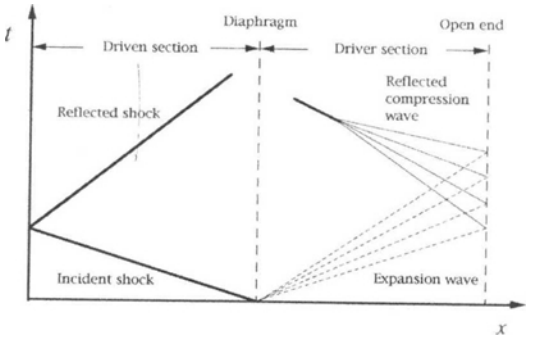

Fig. 2 Wave diagram in the present shock tube

with a diameter of De is installed to exclude the open end correction of the wave phenomena occurring near the shock tube exit. According to the previous work, (Kim et al., 2001a and Kim et al., 2001b) it is known that the baffle plate affects the wave reflection and discharge phenomena from the open end of a duct. In the present study, the diameter of the baffle plate is varied to investigate the baffle plate effect on wave reflection. The initial pressures of the shock tube are monitored by a personal computer system. Calibrated pressure transducers, flush mounted on the shock tube walls at several stations are used to measure and characterize the expansion and compression waves propagating through the tube. Output of the pressure transducer is recorded on an X-Y recorder by way of a wave memory. The pressure transducers are calibrated both statically and dynamically prior to each test. The uncertainty in pressure measurements is estimated to be less than ± 1.5 percent. These estimations are based on the maximum possible fluctuations in the measurements.

3. Computational Analysis

Figure 3 schematically shows the wave diagram

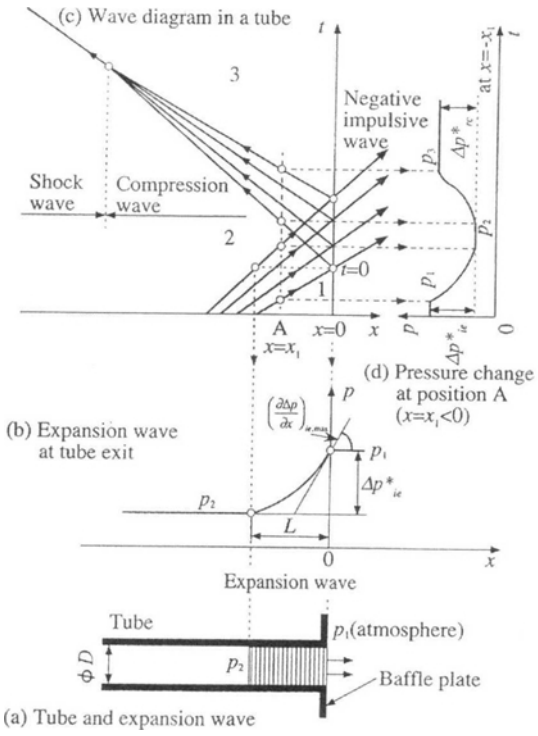

Fig. 3 Schematic diagram of the wave reflection from shock tube exit

to address the reflection phenomenon of an expansion wave near the open-end of the shock tube, together with the symbols used in the present study. When the expansion wave reaches the open end of the shock tube, as shown in Fig. 3(a), some part of the expansion wave is discharged toward the atmosphere, while the rest part of the expansion wave is reflected back as the compression wave from the open end of the shock tube. It is assumed that the pressures behind and before the expansion wave are p_2 and p_1, respectively, as shown in Fig. 3(b), and their difference p_1-p_2 is defined as $\Delta p^*_{ie}(=p_1-p_2)$. The expansion wave length, which is usually the distance between the head and tail of an expansion wave, is assumed by L and the maximum pressure gradient at the expansion wave front is defined by $(\partial \Delta p/\partial x)_{ie,\max}$. In Fig. 3(c), t is defined as the time starting from the instant that the expansion wave head reaches the measurement point A. The expansion wave reflects back as the compression wave from the open end of the shock tube, as

shown in the wave diagram of Fig. 3(c).

Figure 3(d) shows the pressure variation occurring at a location of $x=x_1$. The pressure at the position A ($x=x_2<0$) is kept at a constant value p_1, before the expansion wave reaches the measurement point A. Then it begins to reduce as the head of the expansion wave reaches the measurement point A. The expansion waves reflect back from the exit of the shock tube, leading to a constant pressure p_2 at the point A. Then the pressure rises up to p_3 due to the reflected compression waves at the open end of the shock tube. It is also defined that the pressure difference p_3-p_2 is defined as $\Delta p^*_{rc}(=p_3-p_2)$.

The compression waves will coalesce to be a shock wave inside the tube, as shown in Fig. 3(c). In order to investigate detailed transition processes from compression waves to a shock wave, computations are carried out to simulate the reflection phenomenon of an expansion wave from the open end of the shock tube with an infinite baffle plate at the exit of the shock tube, as shown in Fig. 1. Assuming that air is a perfect gas, the unsteady, axisymmetric, compressible, governing equations can be written in the conservative form ;

$$\frac{\partial U}{\partial t}+\frac{\partial F}{\partial x}+\frac{\partial G}{\partial r}+W=0 \tag{1}$$

$$U=\begin{bmatrix}\rho\\ \rho u\\ \rho v\\ e\end{bmatrix},\ F=\begin{bmatrix}\rho u\\ \rho u^2+p\\ \rho uv\\ (e+p)u\end{bmatrix},$$
$$G=\begin{bmatrix}\rho v\\ \rho uv\\ \rho v^2+p\\ (e+p)v\end{bmatrix},\ W=\frac{1}{r}\begin{bmatrix}\rho v\\ \rho uv\\ \rho v^2\\ (e+p)v\end{bmatrix} \tag{2}$$

where, ρ is the density, u and v are the components of velocity parallel and perpendicular to the tube axis, respectively, p the pressure, e is the sum of the kinetic energy and internal energy per unit volume. In computations, Eq. (1) is rewritten in the dimensionless forms by referring the pressure p_1, density ρ_1, etc, at the atmospheric conditions and the diameter D of the shock tube. The resulting nondimensional form of Eq. (1) is solved numerically using the second order symmetric Total Variation diminishing (TVD) scheme, (Yee, 1987) that is incorporated with the operator splitting technique. (Kim et al., 1999)

A centered-expansion wave given by Eqs. (3) and (4) is assumed to be reflected from the tube exit (Emanuel, 1986),

$$u|_{t=0}=\frac{|x|}{L}u_2 =\frac{|x|}{L}\frac{2}{\kappa-1}\left\{1-\left(\frac{p_1-\Delta p^*_{ie}}{p_1}\right)^{\frac{\kappa-1}{2\kappa}}\right\}a_1 \tag{3}$$

and

$$\frac{p}{p_1}|_{t=0}=\left[1-\frac{|x|}{L}\left\{1-\left(\frac{p_1-\Delta p^*_{ie}}{p_1}\right)^{\frac{\kappa-1}{2\kappa}}\right\}\right] \tag{4}$$

where x means the distance outward from the exit of the tube, as shown in Fig. 3, κ the ratio of specific heats, and a1 is the sound velocity. In the present computations, p_1 is assumed to be 101.7 kPa, and $L/D=1\sim4$, $\Delta p^*_{ie}=4\sim12$ kPa for comparison between the experimental and computational results. Note that the subscripts 1 and 2 used in Eqs. (3) and (4) correspond to the states before and behind the expansion wave, respectively, as illustrated in Fig. 3(c).

The inflow and outflow conditions are applied to the upstream and downstream boundaries, respectively. The symmetric conditions at the centerline of the tube reduce the computational effort for a full domain, and the slip-wall conditions are applied to the solid walls. The upstream boundary is located well back within the shock tube so as to allow for the compression wave to travel back upstream. The downstream boundaries are somewhat varied depending on the value of Δp^*_{ie}, but far enough to avoid the unwanted wave reflections from the boundaries. A square grid system is used to characterize the compression wave reflected from the open end of the tube.

The fineness of computational grid required to obtain grid independent solutions is first examined for some of the expansion waves. The grid density over $\Delta x=\Delta y=D/70$ seems to change the accuracy of obtained solutions no longer. A grid size of $\Delta x=\Delta y=D/75$ is employed in the present computations which ensure that the solutions obtained are independent of the grid density.

4. Results and Discussion

Figure 4 shows the experimental result for pressure variation at the position $x/D=-9.63$, where p_1/p_4 is 1.727 and Δp means the gauge pressure relative to the atmospheric pressure p_1 and D_e/D is the non-dimensional diameter of the baffle plate. The pressure begins to decrease at about $t=0.6$ when the head of the expansion wave reaches the measurement point $x/D=-9.63$, and is kept nearly constant between $t=1.8$ and 4.2. It again rises due to reflections of the expansion waves from the open end of the shock tube. It is very likely that the pressure variation is not significantly influenced by the size of the baffle plate at the exit of shock tube.

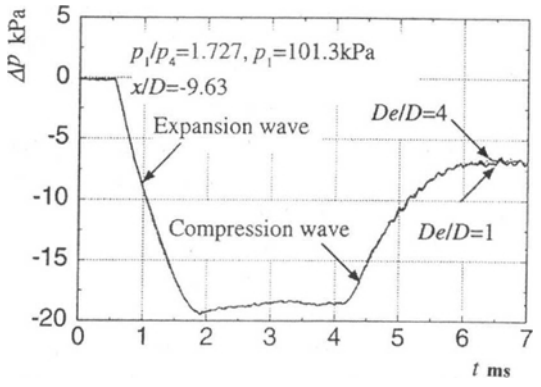

Fig. 4 Experimented results showing the influence of baffle place

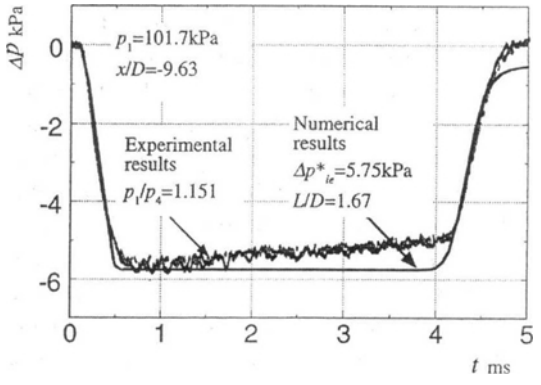

Fig. 5 Comparison between experimented and predicted results of pressure variation at $x/D=-9.36$

Figure 5 shows a comparison between the experimental and computational results of the pressure variations at $x/D=-9.63$. The present computation predicts the experimented pressure history quite well. Some discrepancies are found in the pressure histories between $t=0.5$ and 4.2 ms, and also for $t>4.7$ ms. These are due to boundary layer effects on the pressure histories. At present it is very difficult to predict the ex-

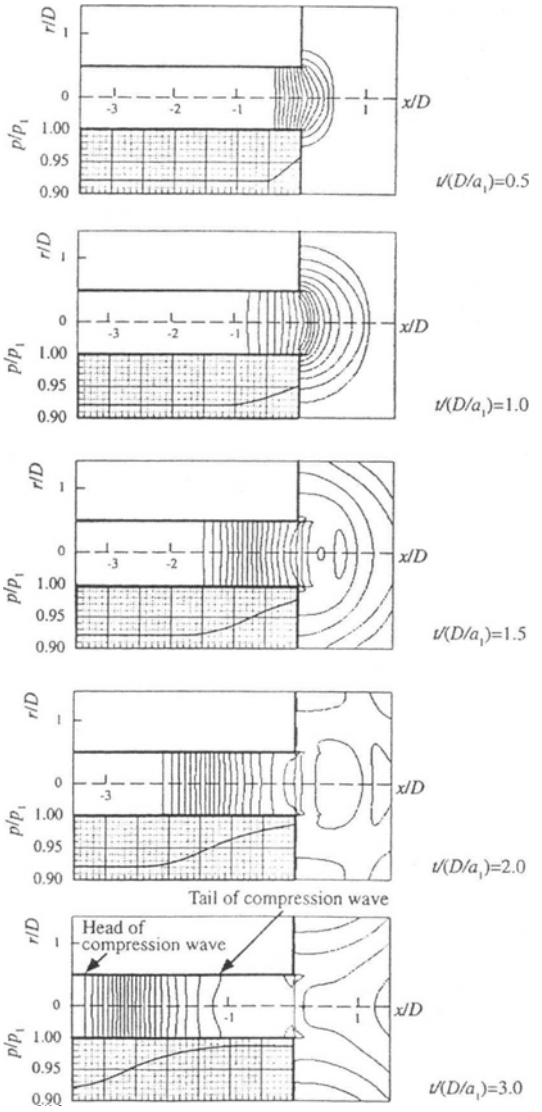

Fig. 6 Computed pressure distributions and contours showing the generation of a compression wave near shock tube exit ($\Delta p^*_{ie}=8$ kPa, $L/D=2$)

pansion and compression wave-induced boundary layer flows. This problem remains unsolved. The boundary layers are generated at the foot of the waves, initially being laminar, but these transit to turbulent flows. This kind of the boundary layer flow is essentially unsteady with a certain singularity inside the wave length.

Typical examples of the predicted pressure contours on the x-r plane are shown in Fig. 6, together with the pressure distributions along the tube axis, where an expansion wave of $\Delta p^*_{ie}/p_1=0.79$ and $L/D=2$ is assumed to be reflected from the open-end of the shock tube at the non-dimensional time $t/(D/a_1)=0$. At $t/(D/a_1)=0.5$, it is found that the compression waves are formed by reflection of the incident expansion waves from the exit of the tube, and the head of the compression waves locates at about $x/D=-0.4$. The compression wave propagate back upstream with time. At $t/(D/a_1)=3.0$, the head of the compression wave locates at $x/D=-3.3$ and the tail at $x/D=-1.2$. From the static pressure distributions along the axis of the tube, it is found that the compression wave front becomes steeper with time. This is due to non-linear effect of the wave itself.

Figure 7 presents the predicted compression wave forms with time, where the incident expansion wave has $\Delta p^*_{ie}=8$ kPa, $p_1=101.7$ kPa and $L/D=2$. Note that the present computation does not involve viscous effects. Thus the magnitude of the compression waves does not change with time. It is interesting to note that the compression wave form becomes gradually steeper with time. For instance, it is found that the compression wave form at $x/D=-47.6$ is much steeper than that at $x/D=-9.5$. In order to investigate the steepness of compression wave form, the maximum pressure gradient of the compression wave front, i.e., the maximum time rate of pressure variation in the compression wave front, is defined as $(\partial\Delta p/\partial t)_{rc,max}$. This parameter is normalized by a proper dimensional quantity of (a_1p_1/D).

Figure 8 shows the relationship between $(\partial\Delta p/\partial t)_{rc,max}/(a_1p_1/D)$ and x/D for several incident expansion waves with different Δp^*_{ie}. For a given value of Δp^*_{ie} it seems that the value of $(\partial\Delta p/\partial t)_{rc,max}/(a_1p_1/D)$ increases with x/D and then it reaches a constant level, depending on the value of Δp^*_{ie}. At a given x/D, the value of $(\partial\Delta p/\partial t)_{rc,max}/(a_1p_1/D)$ increases with Δp^*_{ie}. It is interesting to note that the value of $(\partial\Delta p/\partial t)_{rc,max}/(a_1p_1/D)$ does no longer increase with x/D at the region of $x/D<-50$, regardless of the value of Δp^*_{ie}. The maximum pressure gradient of the compression wave front seems to be saturated at $x/D=50$. This results from the fact that the compression wave becomes a shock wave at this position. The present data show that the position for the compression wave to transit to a shock wave does not depend on the magnitude of the incident expansion wave.

In order to further analyze the compression wave transition to a shock wave, it is defined that

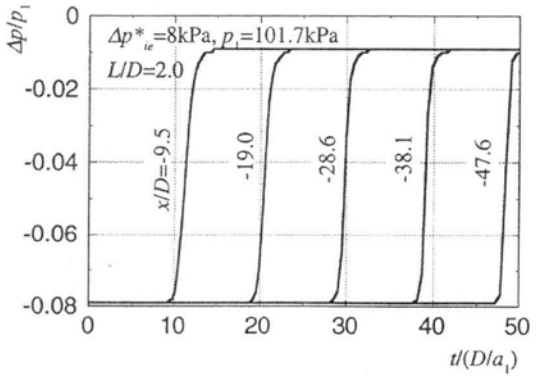

Fig. 7 Maximum pressure gradient of the reflected compression waves

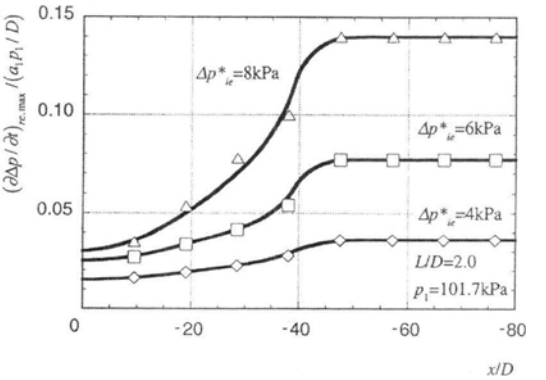

Fig. 8 Relationship between $(\partial\Delta p/\partial t)_{rc,max}/(a_1p_1/D)$ and x/D

the magnitude of the compression wave and its maximum pressure gradient are defined as Δp^*_{rc} and $(\partial \Delta p/\partial t)_{rc,\max}$, respectively, and again the magnitude of the incident expansion wave and its maximum pressure gradient are defined as Δp^*_{ie} and $(\partial \Delta p/\partial t)_{ie,\max}$, respectively, as described in Fig. 3. These parameters can be expressed as the ratio of the reflected compression wave to the incident expansion wave, thus leading to a measure of how much the resulting compression wave is distorted during the propagating processes, as given by Eq. (5),

$$K \equiv \frac{\left(\frac{\partial \Delta p}{\partial t}\right)_{rc,\max} \Big/ \Delta p^*_{rc}}{\left(\frac{\partial \Delta p}{\partial t}\right)_{ie,\max} \Big/ \Delta p^*_{ie}} \tag{5}$$

In Eq. (5), the value of $(\partial \Delta p/\partial t)_{ie,\max}$ is obtained from the relation of a centered-expansion wave, (Emanuel, 1986) as next,

$$\left(\frac{\partial \Delta p}{\partial t}\right)_{ie,\max} = \frac{2\kappa}{\kappa-1}\frac{a_1 p_1}{L}\left\{\left(1-\frac{\Delta p^*_{ie}}{p_1}\right)^{\frac{\kappa-1}{2\kappa}}-1\right\} \tag{6}$$

The value of K defined by Eq. (5) is again plotted against x/D, as presented in Fig. 9, where the magnitude of the incident expansion wave Δp^*_{ie} is varied at a fixed value of L/D. All the data obtained from the present computations are collapsed onto a single curve, leading to good correlations of the present data. Figures 9(a) and (b) show the effect of L/D on the value of K. From both the results it is found that K is essentially independent of the value of Δp^*_{ie}. It is evident that the key factor associated with the compression wave distortion is only the wave length L/D of the incident expansion waves. This conclusion leads to a new correlation as next,

$$\xi \equiv \frac{K-1}{L/D} = \frac{\left\{\frac{(\partial \Delta p/\partial t)_{rc,\max}/\Delta p^*_{rc}}{(\partial \Delta p/\partial t)_{ie,\max}/\Delta p^*_{ie}}\right\}-1}{(L/D)} \tag{7}$$

Figure 10 shows the relationship between the value of ξ defined by the above Eq. (7) and x/L. All the data are again collapsed onto a single curve, leading to a quite good correlation. This indicates that the value of ξ does not depend on L/D and Δp^*_{ie} even when x/L increases. It is evident that the maximum pressure gradient of the

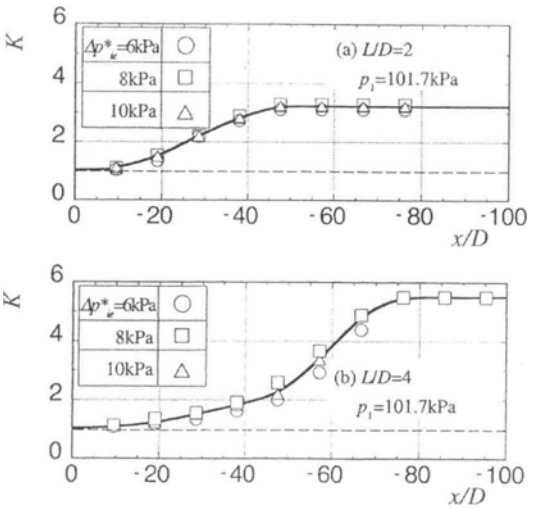

Fig. 9 Relationship between K and x/D

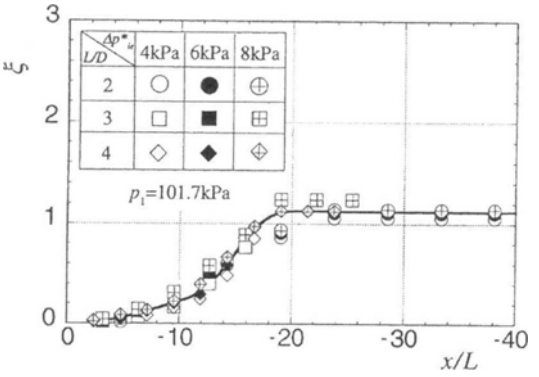

Fig. 10 Relationship between ξ and x/L

reflected compression waves is saturated at the position $x/L=20$, leading to a tendency to transition of the compression wave toward a shock wave. All the present data show that the distance necessary for the reflected compression wave to transit to a shock wave can be found at a location of $x/L=20.0$ regardless of the values of L/D and Δp^*_{ie}.

5. Conclusion

The experimental and computational studies are carried out to investigate the distortion of the compression wave reflected from the open end of a shock tube. Both the experimented and predicted results are in good agreement. The effect of

the size of the baffle plate at the open-end that has on the reflection of the incident expansion wave is found negligible. A good correlation is obtained for transition of the reflected compression wave to a shock wave inside the tube. It is found that the distance necessary for the reflected compression wave to transit to a shock wave does not depend on the magnitude of the incident expansion and its wave length as well. The present data show that for a given wave length of the incident expansion wave transition of the reflected compression wave to a shock wave can be predicted with good accuracy.

Acknowledgment

This work was supported by the Brain Korea 21 project in 2002.

References

Emanuel, G., 1986, "Gasdynamics, Theory and Applications," *AIAA Inc.*, pp. 184~186.

Kentfield, J. A. C., 1993, *Nonsteady, One-Dimensional, Internal, Compressible Flows (Theory and Applications)*, Chapter 7, Oxford University Press.

Kim, H. D., 1996, "Numerical Study on Attenuation and Distortion of Compression Waves Propagating into a Straight Tube," *KSME Journal*, Vol. 20, No. 7, pp. 2315~2325.

Kim, H. D. and Setoguchi, T., 1999, "Study of the Discharge of Weak Shocks from an Open End of a Duct," *Journal of Sound and Vibration*, Vol. 226, No. 5, pp. 1011~1028.

Kim, H. D., Setoguchi, T. and Kashimura, H., 2001(a), "Augmentation of the Magnitude of the Impulsive Wave Discharging from an Open End of a Duct," *IMechE*, Vol. 215, Part C, pp. 191~199.

Kim, H. D., Setoguchi, T. and Kashimura, H., 2001(b), "Study of the Impingement of Impulse Wave upon a Flat Plate," *Journal of Sound and Vibration*, (in press).

Matsuo, K. and Aoki, T., 1992, "Wave Problems in High-Speed Railway Tunnels," *Shock Waves*, Vol. 1, pp. 95~102.

Matsuo, K. and Aoki, K., 1996, "Numerical Study of Attenuation and Distortion of a Compression Wave Propagating in a High-Speed Railway Tunnel," *Computers in Railways V, Vol. 2, Railway Technology and Environmental*, pp. 23~32.

Ogawa, T., 1997, "Numerical Investigation of Three-Dimensional Compressible Flows Induced by a Train Moving into a Tunnel," *Computers and Fluids*, Vol. 26, No. 6, pp. 565~585.

Ozawa, S., 1994, "Distortion of Compression Wave During Propagation Along Shinkansen Tunnel," *proc. 8th Int. Conf. on Aerodynamics and Ventilation of Vehicles*, pp. 221~226.

Raghunathan, S. and Kim, H. D., 1998, "Impulse Noise and Its Control," *Progress in Aerospace Sciences*, Vol. 34, No. 1, pp. 1~44.

Sasoh, A. and Takayama, K., 1993, "A Numerical and Experimental Study of Sonic Booms Generated in High-Speed Train Tunnels," *Shock Waves @ Marseille III*, pp. 353~358.

Yee, H, C., 1987, "Upwind and Symmetric Shock-Capturing Schemes," *NASA Tech. Memo.* 89464.